

IMPACT OF HIGHER FREQUENCY EMISSION ABOVE 2KHZ ON ELECTRONIC MASS-MARKET EQUIPMENT

Jan MEYER, Stephan HAEHLE, Peter SCHEGNER
Technische Universitaet Dresden - Germany
jan.meyer@tu-dresden.de

ABSTRACT

Due to the increasing use of modern technologies (e.g. PWM inverters in PV installations, equipment with active power factor correction circuits, PLC, ...) the emission levels in the frequency range between 2 kHz and 150 kHz are rising continuously. In the recent time the number of reported disturbances (e.g. malfunctions of coffee machines, audible noise of electronic ballasts) caused by this emission is growing. Beside these obvious interferences the question arises, if electronic mass-market equipment is affected by this higher frequency (HF) emission as well. Especially in shunt elements with low impedance at higher frequencies, like DC-link capacitors in rectifier circuits, larger high frequency currents can occur, which may result in additional thermal stress and lifetime reduction.

Based on a laboratory setup the paper analyses the impact of HF components in the supply voltage on the operating temperature within different lamps with electronic ballast. Using a laboratory setup the frequency-dependent input behaviour of different electronic equipment was measured up to 50 kHz. For selected lamps detailed temperature studies were carried out.

INTRODUCTION

The use of power electronics plays an important role in the challenging task of continuous increase of energy efficiency, especially for the mass-market products. The input circuit of this equipment usually contains a rectifier which emits harmonics. Magnitude and frequency range of the harmonic emission is determined by the used rectifier topology. Due to the increasing use of high frequency switching techniques (e.g. in PV inverters or active PFC circuits) a shift of the emission from classical harmonics below 2 kHz to higher frequencies in the range 2 kHz to 150 kHz can be observed. Up to now only few is known about possible impact and propagation of those HF voltages and currents in the grid. Currently virtual no EMC standard exists for this frequency range. The increasing number of interferences linked to higher frequencies (malfunction of equipment, falsification of meter readings, audible noise) urgently requires the development of an appropriate standardization framework consisting of compatibility levels, emission and immunity limits within SC77A [1].

Former research has shown that these HF voltage components will usually not propagate very far in the grid. Other electronic equipment, which is installed in electrically

short distance to the HF emitting source, provides a much better back paths (low impedance) than the grid itself [2]. The low impedance is mainly caused by shunt capacitances that can be part of EMC filters or the DC-link of rectifiers. The crucial importance of capacitors in this issue is also supported by other activities, like a survey on interference cases conducted by SC77A/WG8 or a work on immunity of AC-capacitors in SC77A/WG1.

It is the intention of this paper to do a first step in the systematic analysis of the impact of HF components in particular on the additional thermal stress of electronic equipment. It is mainly, but not exclusively focused on the electrolytic capacitors that are commonly used as DC-link capacitor in rectifier circuits. The analysis is based on measurements using different lamps with integrated electronic ballast as example. The results shall be a contribution to the on-going standard development process by the respective IEC SC77A working groups (WG8, WG6, WG1).

THEORETICAL BACKGROUND

Overview of common rectifier circuits

A wide variety of designs exist for the rectifier circuits that are necessary to convert the AC supply voltage into the internally needed DC voltage at lower voltage level. Fig. 1 gives an overview of the most commonly used technologies. It has to be noted, that especially for active PFC (Power Factor Correction) circuits again a lot of different sub-designs exist.

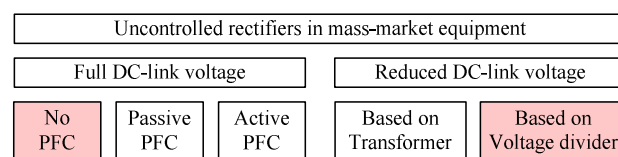


Figure 1 Overview of commonly used rectifier circuits

One central part of all circuits is the DC-link capacitor that provides the smoothed DC voltage to the internal circuit. Circuits without PFC and circuits based on capacitive voltage dividers (highlighted in Fig. 1) represent the simplest design. For both designs the capacitor is directly connected to the grid during the recharging interval. Due to the low impedance at higher frequencies already small voltages can cause significant additional currents at higher frequencies flowing through the capacitor. As an example Fig. 2 shows the input circuit of an 11-W-Compact fluorescent lamp (CFL). The internal circuit of the lamp is usually modelled by an equivalent resistance [3]. The

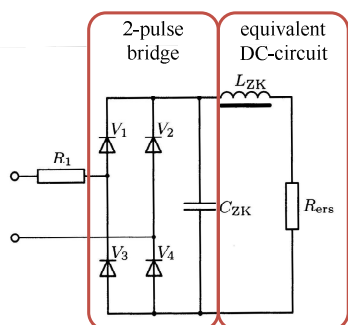


Figure 2 Simplified schematic diagram of a CFL (11W) without PFC

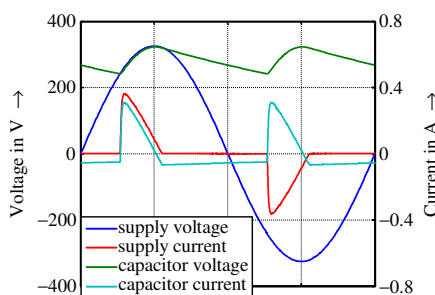


Figure 3 Voltage and current measurement at 230V(50Hz)

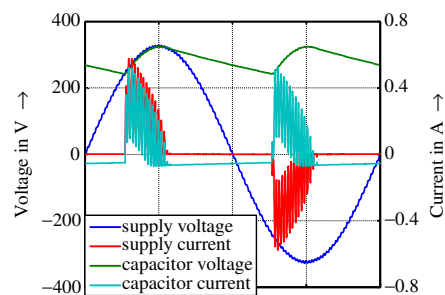


Figure 4 Voltage and current measurement at 230V(50Hz) + 2,3V(5kHz)

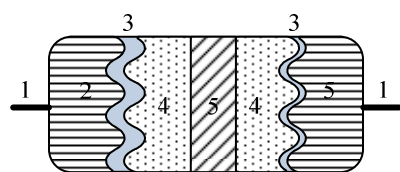
additional HF component in the current flowing through the capacitor can be clearly seen in Fig. 4.

Circuits without PFC have a high harmonic emission up to THDi > 200%. To meet the limits given in IEC 61000-3-2 the application of this circuits is almost limited to lamps with P < 25W and consumer electronics with P < 75W. Equipment with higher input power usually uses more complex circuits (e.g. passive or active PFC). Those circuit designs often contain additional inductive series elements. Due to their increasing impedance at higher frequencies the above described effect is expected to be attenuated.

Therefore the research activities are mainly focused in the first step on equipment without PFC (e.g. CFLs with P ≤ 25W) and capacitive voltage divider (e.g. in LED lamps). The basic design of a capacitive voltage divider consists of an AC capacitor and a DC-link capacitor. In this way the voltage at the rectifier bridge is low. This allows the reduction of the size and the price of the equipment.

Electrolytic capacitors

As discussed in the last chapter the DC-link capacitors in circuits without PFC are mostly affected by HF voltage components. As a rule of thumb the life time of a capacitor is cut in about half by 7 K to 10 K temperature increase. Electrolytic capacitors can be grouped in wet and dry aluminium capacitors, wet and dry tantalum capacitors and dry niobium capacitors. Due to its low price in almost all mass-market applications the wet electrolytic aluminium capacitor is used. Figure 5 shows its principal layout, Figure 6 the respective, already simplified equivalent circuit. According to the equivalent circuit the capacitor is represented by a series resonance circuit with an impedance minimum determined by R_{ESR} and at frequency:



- 1 – connecting leads
- 2 – Aluminium foil (anode)
- 3 – Dielectric (aluminium oxide)
- 4 – Cathode (wet electrolyte)
- 5 – Aluminium foil (cathode lead)

Figure 5 Layout of wet electrolytic aluminium capacitor

$$f_0 = \frac{1}{2\pi\sqrt{C \cdot L_{ESL}}} \tag{1}$$

The impedance curve is specified by the manufacturer in respective data sheets. The location of the minimum ranges from about 10 kHz for a 10000 μF capacitor (data sheet value) up to about 30 kHz for a 10 μF capacitor (own measurement).

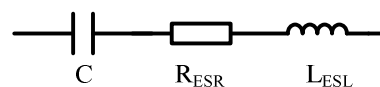
According to the equivalent circuit, only R_{ESR} produces power losses and subsequently generates additional heating. The core temperature rise at current I_B can be calculated based on a reference temperature increase ΔT₀ at a reference current I_R, both provided by manufacturer, to

$$\Delta T_c = \Delta T_0 \frac{I_B^2}{I_R^2} \tag{2}$$

Based on data sheets information and own measurements R_{ESR} reduces with increasing frequency to a minimum value that is about half of its resistance at 100 Hz (DC ripple frequency in 50-Hz-grids). Due to this frequency-dependency of R_{ESR} the different frequency components of the current I_B has to be weighted by frequency-dependent correction factors k_f (data sheet values or measurement). For the capacitors analysed in the paper the minimum value is reached at frequencies of about 1 kHz. A current I_B consisting of multiple frequency components could finally calculated as follows:

$$I_B = \sqrt{\sum_f \left(\frac{V_f / Z_f}{k_f} \right)^2} \tag{3}$$

The applicability of the equation was verified by own lab measurements. For a specific capacitor a core temperature increase of 10K results from a current I_B = 0.55A. Using only a single-frequent ripple of 100 Hz a voltage



- C – capacitance
- R_{ESR} – Equivalent series resistance
- L_{ESL} – Equivalent series inductance

Figure 6 Simplified equivalent circuit

$V_{100\text{Hz}} = 14.4 \text{ V}$ was necessary to get this current. Next a two-frequent ripple consisting of a reduced 100 Hz component and an additional HF component resulting in the same total current $I_B(V_{100\text{Hz}} + V_{\text{xHz}}) = 0.55 \text{ A}$ was applied. Both components contribute 50% each to the total RMS current I_B (0.36 A per component). This was verified for HF components at 1 kHz and 10 kHz. The 100 Hz component amounts always 10.25 V. Due to the decreasing impedance of the capacitor only 1.4 V @ 1 kHz and 0.34 V @ 10 kHz respectively are necessary to get the required 50% contribution to the current I_B by the HF component.

EQUIPMENT INPUT CHARACTERISTICS

According to qualitative considerations, the maximum thermal stress for a particular device can be expected, if the RMS current of the equipment has a maximum too. The input current of a particular device mainly depends on the layout of the input circuit as a whole and not only on the frequency-dependent behaviour of the input impedance of the DC-link capacitor. Therefore in a next step the frequency-dependent input characteristic was studied. Experiences have shown that circuit layout and element parameters differ between manufacturers and lamp models even if the lamps are using the same rectifier technology (e.g. no PFC). Therefore the frequency-dependent input characteristics of 42 different lamps with integrated ballast (29 CFL without PFC, 4 CFL with active PFC, 9 LED lamps) were analysed.

Measurement setup and method

To ensure realistic operating conditions a two-frequent voltage that consists of a fundamental component with 230 V and a HF component with variable magnitude up to 10 % of the fundamental voltage was synthesised by a computer and amplified by a wide-band amplifier (-3 dB @ 150 kHz). Voltage and current signals are sampled with 500 kHz and analysed by an own-developed MATLAB program.

At the beginning of each measurement the RMS current with sinusoidal supply voltage (V_{50}) was measured as reference. Next a HF component (V_{HF}) with 1 % of fundamental voltage was added to the signal and swept from

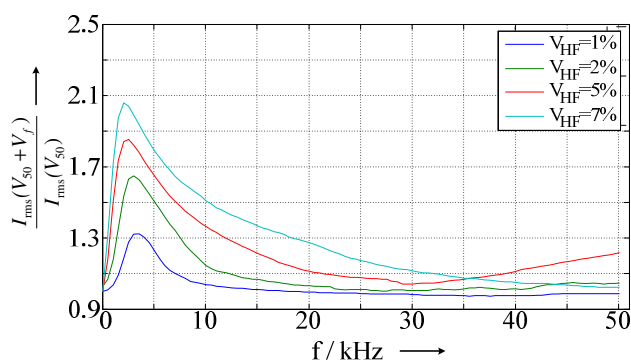


Figure 7 Type A input characteristics measured at a CFL with $P < 25 \text{ W}$

500 Hz to 50 kHz by 500 Hz steps. At each frequency step the respective RMS current was measured. For selected lamps the measurement was repeated using 2 %, 5 % and 7 % of fundamental voltage as HF component.

Measurement results

According to the measurements the analysed lamps generally show two different behaviours (type A and type B) of the input characteristic. Figures 7 and 8 present the frequency dependency of the ratio of the HF component ($I(f)$) to the fundamental component ($I_{50\text{Hz}}$) of the current. The type A behaviour (cf. Fig. 7) is characterized by a distinctive peak of the current ratio at a small frequency range and small values for the other frequencies. The behaviour was observed for some CFLs without PFC. At 1 % HF distortion the maximum ratio varies for the different lamps between slightly above 1 up to 1.35. The maximum occurs in the range between 1 kHz and 5 kHz. The variation is caused by the different circuit layouts and confirms the initially made assumption. A similar behaviour was observed for some of the lamps with active PFC circuit (no diagram shown), but the frequency of the maximum ratio is located between 15 kHz and 20 kHz. It should be noted that the emission of small PV-inverters uses a similar range and may lead to higher interferences with those lamps [4].

The type B behaviour (cf. Fig. 8) is characterized by a large frequency range with significant increased current ratio. This behaviour was observed for the other part of the CFL's without PFC and the LED lamps. It is more critical than the type A one, because the risk that an existing emission matches a frequency with an increased current ratio is much higher. Again a clear dependency of the current ratio from the level of the HF voltage component can be observed. The ratio varies for the different lamps between values only slightly higher than 1 up to more than 2 for a HF voltage of 1 %.

IMPACT ON EQUIPMENT HEATING

Two different CFL's (one without PFC (CFL1), one with active PFC (CFL2)) and one LED lamp (LED1) were selected for a detailed study of the temperature inside the lamps. All lamps were equipped with temperature sensors at

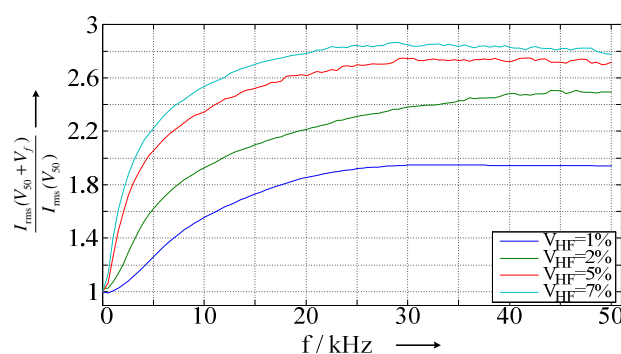


Figure 8 Type B input characteristics measured at a LED lamp with capacitive voltage divider

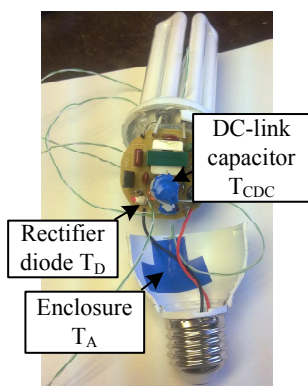


Figure 9 CFL (11W) without PFC (CFL1)

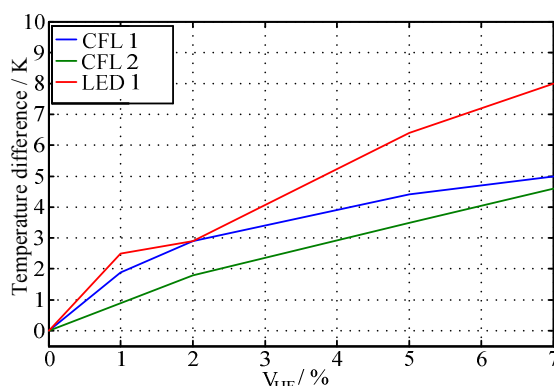


Figure 10 Temperature difference between sinusoidal and distorted supply voltage (DC-link cap.)

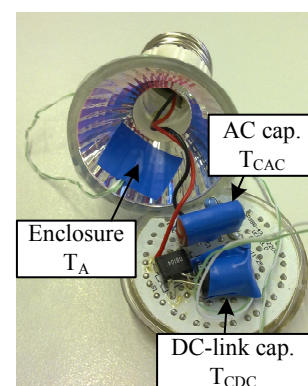


Figure 11 LED lamp with cap. voltage divider

selected points. Fig. 9 and 11 exemplarily illustrate the sensor placement.

As reference case all lamps were supplied with a sinusoidal voltage. In the following measurements a stepwise increased HF voltage was added to the fundamental component at the device-individual frequency of the current ratio maximum:

- CFL1: $I_{rms}(V_{50}+V_{3500})/I_{rms}(V_{50})=1.3$
- CFL2: $I_{rms}(V_{50}+V_{47000})/I_{rms}(V_{50})=1.15$
- LED1: $I_{rms}(V_{50}+V_{30000})/I_{rms}(V_{50})=1.9$

For each measurement always the steady state was awaited for all temperature sensors (about 60 minutes per measurement).

Figure 10 exemplarily shows the temperature difference between two-frequent voltage and reference case depending on the HF voltage level. Selected temperature values are given in Table 1. In most cases not only the temperature of the capacitor increases due to the increased input current, but other elements are affected too.

Environmental temperature was kept constant during all measurements.

Table 1 Selected measured temperature values (for symbol description cf. to Fig. 10 and 12)

	CFL1		CFL2		LED1	
	0%	5%	0%	5%	0%	5%
$T_{CDC}/^{\circ}C$	52.8	57.2	51.5	55.0	45.1	51.5
$T_E/^{\circ}C$	44.0	47.1	70.0	74.1	34.6	38.1
$T_D/^{\circ}C$	76.4	80.1	79.9	80.6	-	-
$T_{CAC}/^{\circ}C$	-	-	-	-	44.1	49.6

CONCLUSIONS

The paper demonstrates that HF voltages can have a significant impact on the thermal stress and subsequently the life time of electronic equipment, which contains rectifiers with electrolytic capacitors as DC link. Especially the equipment without active cooling has shown a significant impact of the HF voltages on operating temperatures. Therefore the discussion about immunity and emission levels should not only consider obvious malfunctions but

also take the possible long-term effects as described in the paper into account.

Besides the additional heating, especially audible noise was observed for a lot of the analysed equipment. This can occur already at HF voltage levels of about 1%.

From the viewpoint of additional thermal stress and disturbing audible noise the compatibility levels in the frequency range up to 20 kHz should be considerably low. Anyway it should be lower than those levels that already cause obvious equipment malfunctions. Moreover it is suggested to introduce a limit for the whole frequency band (similar to THD) too.

Currently the measurements are extended to other equipment (e.g. PC power supplies) and to test voltage waveforms containing more than one HF component. Long-term experiments for an assessment of possible lifetime reductions are planned.

REFERENCES

- [1] Study report on electromagnetic interference between electrical equipment / systems in the frequency range below 150 kHz. CENELEC SC 205A mains communication systems, Taskforce EMI, 01/2009.
- [2] S. Rönnerberg, M. Wahlberg, M. Bollen, A. Larsson, M. Lundmark: "Measurements of interaction between equipment in the frequency range 9 to 95 kHz", CIRED conference, Session 2, June 2009, Frankfurt a.M., Germany.
- [3] A.J. Collin, J.L. Acosta, B.P. Hayes, S.Z.Djokic: "Component-based aggregate load models for combined power flow and harmonic analysis", (MedPower 2010), November 2010, Agia Napa, Cyprus.
- [4] M. Klatt, J. Meyer, P. Schegner, C. Körner, G. Eberl, T. Darda: "Emission levels above 2kHz - laboratory results and survey measurements in public low voltage grids", CIRED conference, June 2013, Stockholm, Sweden.